Simple demonstration of the intermediate axis theorem with a Smartphone based example, numerical and experimental results.

C. J. Pereyra, M. Osorio, A. Laguarda and D. L. Gau

Instituto de Física, Facultad de Ingeniería, Universidad de la República, Julio Herrera y Reissig 565, Montevideo, Uruguay.

Correspondence author: jpereyra@fing.edu.uy (CJP); mosorio@fing.edu.uy (MO)

Abstract

A combination of numerical calculations and smartphone based demonstrative experiment is used to demonstrate the intermediate axis theorem. The differences in the dimensions of the smartphone are used to observe the theorem. For every initial condition a very good agreement is obtained between the numerical solution and the experimental results. The implemented methodology proven to be a good demonstration of a rather complex phenomena.

Introduction

In last years, smartphones become a a massive and powerful tool to perform live demonstration of several physical phenomena in the classroom, mainly due to its capacity of acquire and present a high volume of data in real time obtained from different sensors inside the phone. This provides a simple way to create a wide variety of experimental setups. Different useful demonstrations for classical mechanics were performed in this way to study topics of classical mechanics such as dynamics and energy of a rigid body in a circular movement [1–3], angular momentum [4] and angular velocity [5–7]. Also, this tool opens a broad band of opportunities to study various phenomena based on experiences of daily life, like the ones reported in [8,9], or acoustic waves and sound analysis [10,11].

When presented in undergraduate classroom topics like kinematic and dynamics of rigid body, movement restricted both to a plane or space, have an inherent complexity, mainly due to difficulties in the visualization of different movements and preconceptions about the movements by the students. In this paper, we present a simple and low-cost demonstration to be used in the classroom for the study of a rotational rigid body in space. One of the most uncommon characteristic of these dynamical examples is the so called intermediate axis effect also known as tennis racket effect or Dzhanibekov effect [12–17], recently presented on Youtube channel Veritasium [18]. In order to demonstrate this effect, free rotations on the three different inertial axis of a smartphone are studied. The experimental results are compared with the numerical solutions for the angular velocity of the rigid body.

We use a smartphone (which can be modeled as a thick rectangular plate) as the rigid body with three different moments of inertia and data logger at same time, and, combined with a simple analysis, allow us to determine the angular velocity of the system and compare it with the expected behavior from the numerical solution.

Theoretical background

Inertia Tensor for a 3-D rigid body

For a 3-D rigid body with the shape of a cuboid (e.g. thick rectangular plate), the inertia tensor in a set of eigenvectors of the rigid with respect to it center of mass G (see Figure 1) exhibits a diagonal form [17]:

$$\mathbb{I}_G = \begin{pmatrix} I_1 & 0 & 0 \\ 0 & I_2 & 0 \\ 0 & 0 & I_3 \end{pmatrix} \qquad (1)$$

Where I_1, I_2 and I_3 are the inertia moments among their respective principal axes where the values of the inertia moments are determinate by the shape and mass distribution of the body.
Let consider the smartphone as a homogeneous rectangular cuboid of mass m (as showed in Fig. 1) and its center of mass G. If the coordinate systems of the principal axes of inertia for the plate (in Fig. 1 named as $\hat{e}_1, \hat{e}_2$ and $\hat{e}_3$, respectively) is used, then, the inertial tensor has a diagonal form:

$$\mathbb{I}_G = \frac{m}{12}\begin{pmatrix} W^2 + t^2 & 0 & 0 \\ 0 & L^2 + t^2 & 0 \\ 0 & 0 & L^2 + W^2 \end{pmatrix} (2)$$

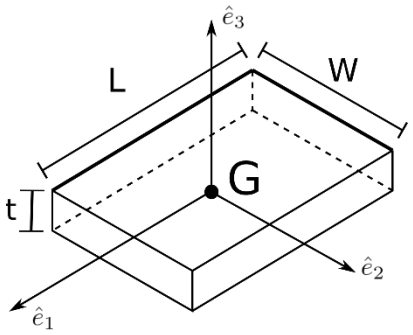

Figure 1: Example of the system to be analyzed, which is based on a thick rectangular plate that can rotate freely.

Due to the shape of the smartphone and the relation between its length (L), width (W) and thickness (t) the inertia moments will follow the following relation $I_1<I_2<I_3$, therefore I_2 will be the intermediate axis of the rigid. The angular velocity of the rigid will be defined as $\vec{\omega} = \omega_1\hat{e_1} + \omega_2\hat{e_2} + \omega_3\hat{e_3}$ where each $\hat{e_i}$ $i=1,2,3$, are the same axis of the rigid as defined in Figure 1.
In order to understand the Intermediate axis Theorem Effect (ITE), the Euler equations (based on the reference system mentioned above) should be addressed [17]:

$$\begin{aligned} I_1\dot{\omega}_1 &= (I_2 - I_3)\omega_2\omega_3 \\ I_2\dot{\omega}_2 &= (I_3 - I_1)\omega_1\omega_3 \\ I_3\dot{\omega}_3 &= (I_1 - I_2)\omega_1\omega_2 \end{aligned} \quad (3)$$

To achieve the objective of analyze the full behavior of the angular velocities for the rigid body, the system of equations (3) should be solved. Several works were devoted to the full resolution of the system and the evaluation of the stability of the solutions [12–16]. Despite the fact that some approximations can be made [17] in order to simplify the calculations, in this work the solution were obtained by the numerical integration of the set of equations (3), using Matlab. Several different solutions could be obtained by changing the initial condition on the angular velocities $\omega(0) = \omega_1(0)\,\hat{e_1}(0) + \omega_2(0)\,\hat{e_2}(0) + \omega_3(0)\,\hat{e_3}(0)$ (in short notation $\boldsymbol{\omega}(0)=[\omega_1(0), \omega_2(0), \omega_3(0)]$).

Remembering that $I_1<I_2<I_3$ and without the need of obtaining the exact solutions of the equations of motion, three limits for the movement of the system will be studied for short times close to the experimental initial conditions.
In order to achieve a good comparison with the experimental results, the initial conditions for the numerical integration of the equations (3) were selected in accordance with the experimental initial conditions. Moreover, the initial conditions for the simulations ($t_{num}=0$) were selected following the observed experimental values at the beginning of each set of experimental data.

Experimental setup and measurements

The experimental setup consisted on a smartphone (iPhone SE 2nd generation), which played the role of the rectangular cuboid and datalogger. The smartphone was used to measure the angular velocity on each of the principal axis of the smartphone at real time by the accelerometer gyroscope sensor (a detailed explanation of the influence of the position of the gyroscope sensor in the smartphone can be found in [19]). The access of the data sensor was via the app Physics Toolbox Sensor Suite [20]. The data were saved in a CSV file, and sent to a PC in which a post-processing step was performed.

In order to obtain the different torque free rotations, the smartphone was tossed into the air with an specific initial condition $\boldsymbol{\omega}(0)$. In order to observe the phenomena certain vertical velocity v_0

was also applied to the smartphone to obtain a time span of $t = {}^{2v_0}/_{g}$ where g is the modulus of the gravity acceleration. The smartphone was initially set in a vertical and rotational motion; the rotational motion was carefully set to match the pure rotation initial conditions around each principal axis of the smartphone. However, small perturbations were expected due to the difficulty to set a specific pure rotation. These small perturbations will aid to the observation of the different cases under study and to observe the ITE. As the data acquisition starts before the smartphone is set on movement the initial condition occurs at an instant $t_{exp}=t_0\neq 0$. Therefore, after the numerical integration a time translation is applied in order to show the same time expand for both the numerical solution and the experimental results (i.e. $t_{num}= t_{exp}-t_0$).

Six measurements were conducted. First, we set the smartphone in both vertical (against gravity force) and rotational motion with an angular velocity ω_0 mainly respect to $\hat{e}_1$ ($\boldsymbol{\omega}(0)=[\omega_0, \omega_2(0), \omega_3(0)]$) this was named Case 1. Then, a second motion was set, with a rotation of ω_0 mainly respect to $\hat{e}_2$ ($\boldsymbol{\omega}(0)=[\omega_1(0), \omega_0, \omega_3(0)]$) named as Case 2. Finally, the rotation of the smartphone was set in rotation mainly respect to $\hat{e}_3$ ($\boldsymbol{\omega}(0)=[\omega_1(0), \omega_2(0), \omega_0]$) named as Case 3. For each case two experiments were implemented: experiments with rather small ω_0 values were imposed to the smartphone (experiment a) and experiments where higher angular velocities were used (experiment b).

For all the cases and experiments a vertical velocity was also applied to the smartphone, the data acquisition took place until the smartphone reached the same initial height (with respect to the laboratory). Although, the rotation motion was mainly imposed with respect to the desired axis in each case, small rotations with respect to the other axis were also imposed (i.e. $\omega_1(0)$, $\omega_2(0)$ and $\omega_3(0)$ were nonzero) these different values allowed to the visualization of the phenomena and are particularly needed to observe the ITE [13,15,16].

Results and discussion

Experimental results for the Case 1 are presented in Figure 2a and 2c. For both low and high initial angular velocities ω_0 respectively, the angular velocities along $\hat{e}_2$ and $\hat{e}_3$ ($\omega_2(t)$ and $\omega_3(t)$) presents oscillations as expected from equations (3). Moreover, $\omega_1(t)$ also presents an oscillation with time according with the mixed nature of the Euler equations. These results are very well reproduced by the numerical solution of equations (3) as observed in Figures 2a and 2b respectively. By comparing both low and high initial angular velocities a change in the frequency of the oscillations could be inferred, this topic will be covered in detail below.

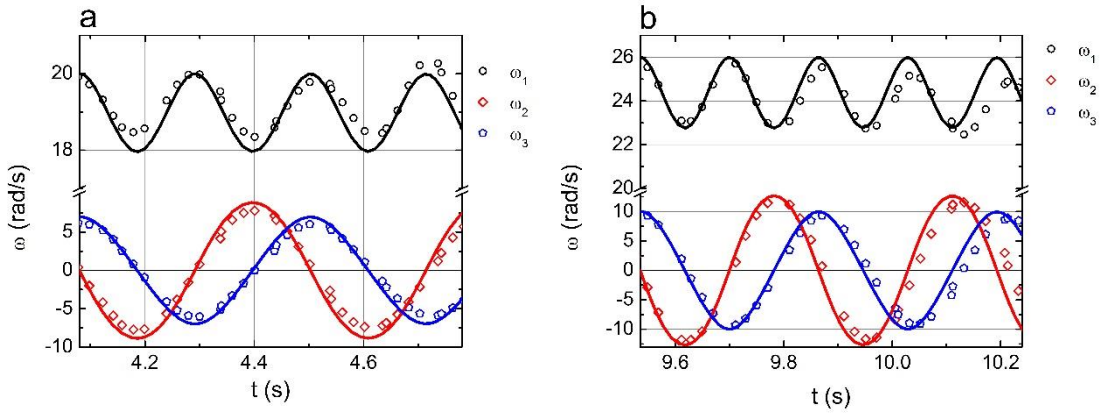

Fig. 2. Angular velocities for Case 1 for: Experiment a (subfigure a) and Experiment b (subfigure b). Angular velocity on $\hat{e}_1$ (black circles), on $\hat{e}_2$ (red diamonds) and on $\hat{e}_3$ (blue

pentagrams). Numerical solutions of Euler equations for the same initial conditions are expressed in full lines.

The symmetric behavior could be observed for Case 3 in Figure 3. In this case, pure rotation among $\hat{e}_3$ was imposed. A very similar behavior than for Case 1 is obtained. The obtained oscillations follows the same conduct than the previously discussed ones. Also, an increase in the frequency of the oscillations on $\omega_1(t)$ and $\omega_2(t)$ is also observed.

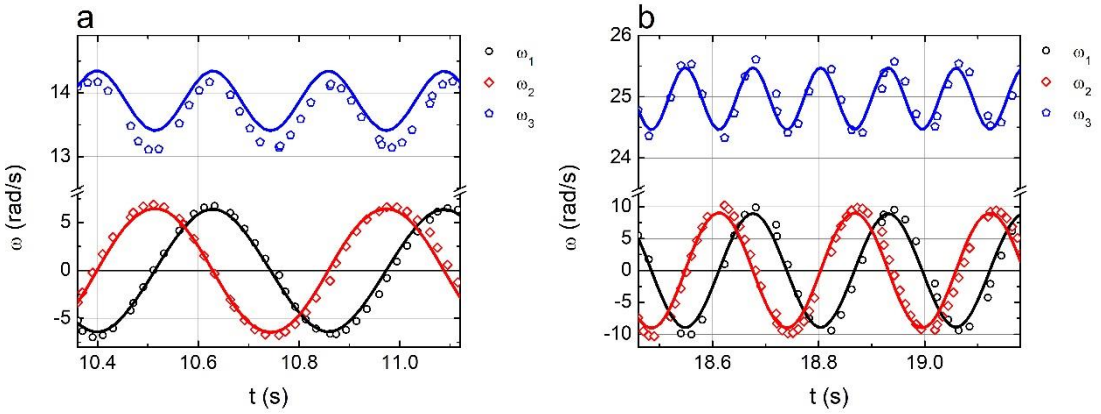

Fig. 3. Angular velocities for Case 3: Experiment a (subfigure a) and Experiment b (subfigure b). Angular velocity on $\hat{e}_1$ (black circles), on $\hat{e}_2$ (red diamonds) and on $\hat{e}_3$ (blue pentagrams). Numerical solutions of Euler equations for the same initial conditions are expressed in full lines.

Finally, the period of the oscillations in $\omega_2(t)$ and $\omega_3(t)$ for Case 1, and $\omega_1(t)$ and $\omega_2(t)$ for Case 3 are presented in Table 1. A very good agreement between the experimental and numerical solutions is obtained. Moreover, from the comparison between Experiment a and b, the increase in the frequency of the oscillations observed in Figures 2 and 3 is confirmed. Higher values of ω_0 lead to smaller periods of the oscillations.

Case	$T_{numerical}$ (s)	$T_{experimental}$ (s)
Case 1a	0.42 ± 0.01	0.43 ± 0.01
Case 1b	0.33 ± 0.01	0.34 ± 0.01
Case 3a	0.46 ± 0.01	0.48 ± 0.01
Case 3b	0.26 ± 0.01	0.26 ± 0.01

Table 1. Period of the oscillations of the angular velocity ω_2 for the Cases 1 and 3 with both initial conditions.

Finally for the observation of the intermediate axis theorem effect, rotations among $\hat{e}_2$ were imposed onto the smartphone. For a complete set of observations, several cases were studied. Cases presented in Figure 3 are rotations with low values of $\omega_1(0)$ and $\omega_3(0)$ for both small (Figure

3a) and high (Figure 3b) initial angular velocities $\omega_2(0)$. The ITE is clearly observed in the change of sign of $\omega_2(t)$ which represent the flip of the smartphone. These variations are periodic in time in accordance with previously reported results [15,16]. Moreover, the frequency of the oscillations seems to increase with the increase in $\omega_2(0)$. The plateaus in $\omega_2(t)$ corresponds with the rotation mainly on $\hat{e}_2$ the flip in $\hat{e}_2$ occurs when both $\omega_1(t)$ and $\omega_2(t)$ reach their maximum absolutes values. As the angular velocities increases the time duration of the plateaus decreases in accordance with the increase in the angular velocities $\omega_1(t)$ and $\omega_2(t)$. Finally, a very good agreement with the numerical solution of the Euler equations is also obtained.

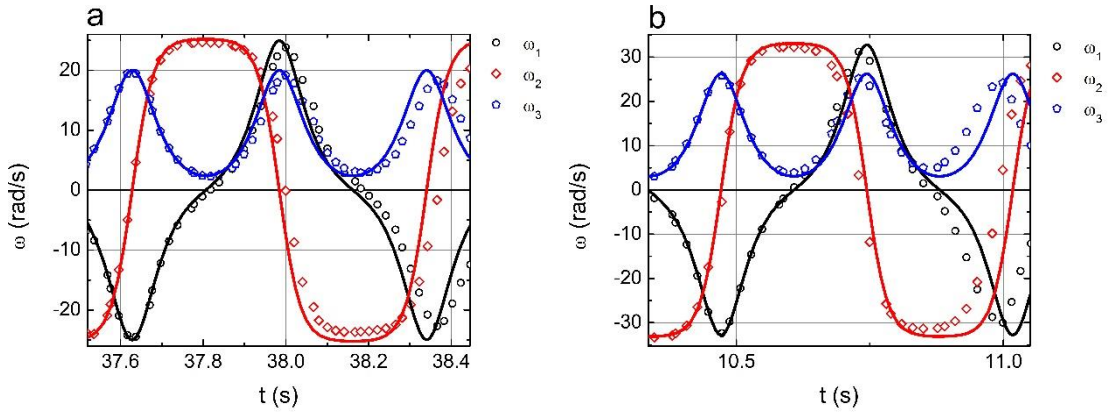

Fig. 4. Angular velocities for Case 2 Experiment a (subfigure a) and Experiment b (subfigure b). Angular velocity on $\hat{e}_1$ (black circles), on $\hat{e}_2$ (red diamonds) and on $\hat{e}_3$ (blue pentagrams). Numerical solutions of Euler equations for the same initial conditions are expressed in full lines.

Further insight into the phenomena is observed by changing the initial values of the other components of the angular velocity $\omega_3(0)$. These results are presented in Figure 5, in this case a higher value of $\omega_3(0)$ was used, a faster flip dynamic is obtained. The time duration between the flips in $\omega_2(t)$ is further reduced until almost no plateaus are observed.

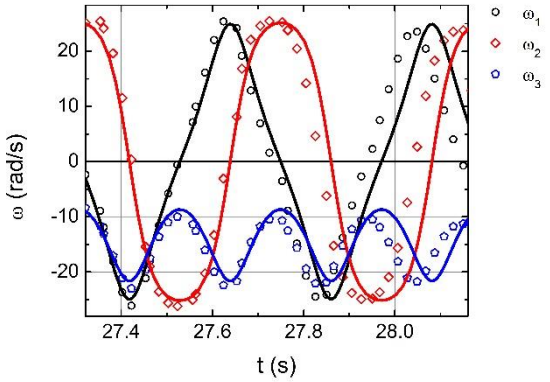

Fig. 5. Angular velocities for Case 2, with higher initial conditions. Angular velocity on $\hat{e}_1$ (red diamonds), on $\hat{e}_2$ (black circles) and on $\hat{e}_3$ (blue pentagrams). Numerical solutions of Euler equations for the same initial conditions are expressed in full lines.

Conclusions

A very simple demonstration of the intermediate axis theorem of a rigid body in a torque free rotation was presented. The experimental set-up is easy to construct and with a small data processing stage the differences between each case are clearly observed. Moreover, a numerical solution of the equations of motions could be obtained for the experimental system. A very good agreement between the expected periods of oscillations of the angular velocities and the experimental results were obtained. Despite the small-time span of the phenomena up to three flips in the $\omega_2(t)$ are observed. The experiment could be a very valuable tool to be used in general mechanics and laboratory courses, in order to study and visualize the kinematics of the free rotations of a rigid body, allowing to the observation of a non obvious behavior.

Acknowledgments

The authors wish to thank the Programa de Desarrollo de las Ciencias Básicas (PEDECIBA), the Comisión Sectorial de Investigación Científica (CSIC) and the Agencia Nacional de Investigación e Innovación (ANII).

References

[1] A. Shakur and J. Kraft, Phys. Teach. **54**, 288 (2016).

[2] Z. Yan, H. Xia, Y. Lan, and J. Xiao, Phys. Educ. **53**, 015011 (2018).

[3] M. Monteiro, C. Cabeza, and A.C. Marti, Phys. Teach. **52**, 180 (2014).

[4] A. Shakur and T. Sinatra, Phys. Teach. **51**, 564 (2013).

[5] M. Patrinopoulos and C. Kefalis, Phys. Teach. **53**, 564 (2015).

[6] V.L.B. de Jesus, C.A.C. Pérez, A.L. de Oliveira, and D.G.G. Sasaki, Phys. Educ. **54**, 015003 (2019).

[7] M. Monteiro, C. Cabeza, A.C. Marti, P. Vogt, and J. Kuhn, Phys. Teach. **52**, 312 (2014).

[8] R.E. Vieyra and C. Vieyra, Phys. Teach. **52**, 149 (2014).

[9] A.-M. Pendrill and C. Modig, Phys. Educ. **53**, 045017 (2018).

[10] M. Osorio, C.J. Pereyra, D.L. Gau, and A. Laguarda, Eur. J. Phys. **39**, (2018).

[11] C.J. Pereyra, M. Osorio, A. Laguarda, and D.L. Gau, Phys. Educ. **53**, 045019 (2018).

[12] L. Van Damme, P. Mardešić, and D. Sugny, Phys. D Nonlinear Phenom. **338**, 17 (2017).

[13] R.H. Romer, Am. J. Phys. **46**, 575 (1978).

[14] T.J. Impelluso, 1 (2015).

[15] A. Amengual, Am. J. Phys. **64**, 82 (1996).

[16] H. Murakami, O. Rios, and T.J. Impelluso, J. Appl. Mech. Trans. ASME **83**, (2016).

[17] H. Goldstein, C.P. Poole, and J.L. Safko, *Classical Mechanics* (Addison Wesley, 2002).

[18] Veritasium, (2019).

[19] V.L.B. de Jesus, C.A.C. Pérez, A.L. de Oliveira, and D.G.G. Sasaki, Phys. Educ. **54**, 015003 (2019).

[20] Vieyra Software, (2017).